

Communication

# Solution-Processed CdTe Thin-Film Solar Cells Using ZnSe Nanocrystal as a Buffer Layer

Yanru Chen <sup>1,†</sup>, Xianglin Mei <sup>1,†</sup>, Xiaolin Liu <sup>1,†</sup>, Bin Wu <sup>1,†</sup>, Junfeng Yang <sup>1,†</sup>, Junyu Yang <sup>2</sup>, Wei Xu <sup>1,3,\*</sup>, Lintao Hou <sup>2,\*</sup>, Donghuan Qin <sup>1,3,\*</sup>  and Dan Wang <sup>1,3</sup>

<sup>1</sup> School of Materials Science and Engineering, South China University of Technology, Guangzhou 510640, China; caro\_ccyr@163.com (Y.C.); depueedome@gmail.com (X.M.); liulin9708@163.com (X.L.); wubin868888@163.com (B.W.); yjf\_yang@126.com (J.Y.); wangdan@scut.edu.cn (D.W.)

<sup>2</sup> Guangdong Provincial Key Laboratory of Optical Fiber Sensing and Communications, Siyuan Laboratory, Guangzhou Key Laboratory of Vacuum Coating Technologies and New Energy Materials, Department of Physics, Jinan University, Guangzhou 510632, China; junyuyang1992@163.com

<sup>3</sup> Institute of Polymer Optoelectronic Materials & Devices, State Key Laboratory of Luminescent Materials & Devices, South China University of Technology, Guangzhou 510640, China

\* Correspondence: xuwei@scut.edu.cn (W.X.); thlt@jnu.edu.cn (L.H.); qindh@scut.edu.cn (D.Q.); Tel.: +86-020-8711-4346 (W.X.); +86-020-8522-4386 (L.H.); +86-020-8711-4346 (D.Q.)

† These authors contributed equally to this work.

Received: 9 July 2018; Accepted: 16 July 2018; Published: 21 July 2018



**Abstract:** The CdTe nanocrystal (NC) is an outstanding, low-cost photovoltaic material for highly efficient solution-processed thin-film solar cells. Currently, most CdTe NC thin-film solar cells are based on CdSe, ZnO, or CdS buffer layers. In this study, a wide bandgap and Cd-free ZnSe NC is introduced for the first time as the buffer layer for all solution-processed CdTe/ZnSe NC hetero-junction thin-film solar cells with a configuration of ITO/ZnO/ZnSe/CdTe/MoO<sub>x</sub>/Au. The dependence of the thickness of the ZnSe NC film, the annealing temperature and the chemical treatment on the performance of NC solar cells are investigated and discussed in detail. We further develop a ligand-exchanging strategy that involves 1,2-ethanedithiol (EDT) during the fabrication of ZnSe NC film. An improved power conversion efficiency (PCE) of 3.58% is obtained, which is increased by 16.6% when compared to a device without the EDT treatment. We believe that using ZnSe NC as the buffer layer holds the potential for developing high-efficiency, low cost, and stable CdTe NC-based solar cells.

**Keywords:** solution processed; CdTe; ZnSe; nanocrystal; solar cells

## 1. Introduction

Solution-processed thin-film solar cells based on nanocrystals (NC), perovskites, or organic light absorbers have many merits such as low cost, easy large-area manufacturing, flexibility and high efficiency, which make them competitive when compared with traditional crystal Si or thin-film solar cells based on vacuum technics [1–7]. Among different kinds of NCs, CdTe NC solar cells have attracted greater attention in recent years [8–11]. CdTe possesses an idea bandgap of ~1.45 eV and a large absorption coefficient ( $>10^4$ /cm in the visible region), which are promising with regard to achieving impressive power conversion efficiency (PCE). Nowadays, CdTe thin-film solar cells with efficiency  $>22\%$  has been realized by optimizing the fabricating techniques, while other thin-film solar cells such as CuIn<sub>x</sub>Ga<sub>(1-x)</sub>Se<sub>2</sub> (CIGS) or perovskite with efficiency up to 23% are also realized, which is prospective for low-cost and efficient solar cell products [12]. By contrast, with the development of NC thin film treatment technics and device structure design, the PCE of solution-processed CdTe

NC solar cells has been elevated to ~12% with a normal structure of ITO/CdTe/In:ZnO/Al [13–15], which shows potential compared with amorphous Si solar cells. However, in most cases, in order to obtain a PCE up to 10%, a light/voltage treatment must be taken out before the device measurement in order to eliminate the energy barrier between the ITO and the CdTe active layer. Therefore, device stability is a vital issue in this case. It has been recently reported that stable and efficient CdTe NC/ZnO solar cells with a configuration of ITO/ZnTe/CdTe/In:ZnO/Al can be attained by inserting a thin layer of ZnTe:Cu, etched CdTe:Cu or Te buffer layer between CdTe and ITO [16]. For CdTe NC solar cells with an inverted structure, satisfactory ohmic contact between the CdTe and the metal can be realized by adopting metals and metal oxides as well as an organic hole transport layer for collecting holes [17]. The most successful CdTe NC solar cells with inverted structures using CdSe, CdS, or TiO<sub>2</sub> buffer layers have been well developed. Crisp et al. developed CdTe NC solar cells by using chemical bath deposition (CBD) CdS [18] as the electron acceptors. A PCE as high as 6.66% is obtained in this case. It has also been found that the substitution of CdS NC for CBD–CdS can improve the quality of the CdTe/CdS hetero-junction and suppress the dark current [19]. Following this, CdTe/CdSe NC solar cells with inverted structures such as ITO/CdSe/CdTe/Au were developed and improved performance was demonstrated [20]. Later, the CdTe:CdSe NC hybrid layer and the graded-bandgap structure designs were introduced into the CdTe/CdSe NC solar cells. Additionally, PCEs of 6.25% and 6.34% were achieved in device structures of ITO/ZnO/CdSe/CdSe:CdTe/CdTe/Au and ITO/ZnO/CdSe/CdSe<sub>x</sub>Te<sub>1-x</sub>/CdTe/MoO<sub>x</sub>/Au, respectively [21,22]. More recently, a novel cross-linkable conjugated polymer has been applied as the hole transport layer (HTL) for CdTe NC solar cells and a very high PCE of 8.34% obtained with the structure of ITO/ZnO/CdSe/CdTe/HTL/Au due to the reduced recombination in the back contact and the interface dipole effect [23]. It is noted that the incorporation of CdSe (with thickness below ~100 nm) is helpful in enhancing the short-circuit current due to the easy formation of CdSeTe alloy with low bandgap and the reduced interface recombination. The formation of CdSeTe alloy will increase the external quantum efficiency spectrum (EQE) response both in the short wavelength and long wavelength regions, which has been confirmed in the literature and our previous reports [22,24,25]. However, CdSe thickness up to 100 nm will result in low device performance due to incomplete formation of CdSeTe alloy. TiO<sub>2</sub> is also found to be a good n type partner for CdTe NC solar cells. Yang et al. [26] fabricated CdTe-TiO<sub>2</sub> heterojunction solar cells by introducing p type spiro-OMeTAD as the hole transport layer for hole collecting. Yang et al. obtained a PCE coupled with 0.71 V of  $V_{oc}$  as high as 6.56%. The  $V_{oc}$  of NC solar cells was further improved when the Sb-doped TiO<sub>2</sub> was used as the electron acceptor material instead of the un-doped TiO<sub>2</sub> [27]. It is noted that CdSe or CdS is low bandgap semiconductor (about 1.8 eV for CdSe and 2.4 eV for CdS), which will render the spectrum response in a short wavelength for CdSe (or CdS) NC thickness up to 100 nm. Therefore, it is necessary to quickly develop new electron acceptor materials with a wide bandgap for the further commercial application of CdTe NC thin-film solar cells. Compared to CdS or CdSe, ZnSe is a wide bandgap (2.7 eV) and Cd-free semiconductor. Therefore, it is expected that the short wavelength response of CdTe solar cells will be improved using ZnSe buffer layer materials since it allows more light to pass without being absorbed. Sputtering ZnSe thin film was applied as a buffer layer successfully in CdTe thin-film solar cells [28,29] prepared by the close space sublimation method. However, there is still no report on CdTe NC solar cells with a ZnSe NC buffer layer prepared by solution-processing.

In this paper, we report on the synthesis of high-quality ZnSe NC using the hot injection method. Devices with a structure of ITO/ZnO/ZnSe/CdTe/MoO<sub>x</sub>/Au were fabricated through layer-by-layer sintering. The effects of ZnSe NC thickness, the annealing temperature, and ligand treatment on the NC solar cells were investigated in detail. Our research study illuminates that, compared to devices without 1,2-ethanedithiol (EDT) treatment, higher  $V_{oc}$  and PCE can be attained in devices with EDT treatment, which accounts for the low defect intensity and high junction quality.

## 2. Experimental Procedure

### 2.1. Materials

Zinc oxide (ZnO), myristic acid ( $C_{14}H_{28}O_2$ ), cadmium nitrate tetrahydrate ( $H_8CdNO_7$ ), pyridine ( $C_5H_5N$ ), methanol ( $CH_4O$ ), 1-hexadecylamine (HDA), tri-n-octylphosphine, tellurium powder, sodium hydroxide (NaOH), ethanolamine, 2-methoxyethanol, and zinc acetate were purchased from Aladdin, Shanghai, China. All other chemicals and solvents were used as received.

### 2.2. Nanocrystal (NC) Synthesis

The ZnO precursor and CdTe NCs synthesis is similar to methods reported previously [10]. ZnSe NCs were fabricated by using the hot injection method with ZnO as a precursor [30,31]. A typical synthetic procedure includes adding 2 mmol (0.1644 g) zinc oxide, 10 mmol (2.3068 g) myristic acid, 16 mmol HDA (4.2926 g) into a three-necked flask. The mixture was heated to 300 °C at a heating rate of 15 °C for 10 min under nitrogen flow. The mixture was kept at 300 °C for 15 min. After that, TOP-Se (2 mL, 1 mmol/mL) was quickly injected into the reaction flask. After injection, the mixture was kept at 280 °C for another 30 min and was cooled gradually to room temperature. The ZnSe NC is precipitated using methanol and was then centrifuged. This process is repeated three times and the CdTe NC is refluxed in pyridine for 12 h and centrifuged with hexane. The final product is dispersed into a mixture of pyridine and 1-propanol with a volume ratio of 1:1 at about 50 mg/mL.

### 2.3. Device Fabrication

The solar cells with the inverted structure of ITO/ZnO/ZnSe/CdTe/MoOx/Au are fabricated by using a layer-by-layer solution process. First, the ZnO precursor is deposited on ITO substrate and annealed at 400 °C for 10 min to eliminate any organic solvent and allow the formation of the ZnO thin film with a thickness of ~40 nm. Several drops of ZnSe NCs solution are then put on top of the ITO/ZnO substrate and spin-casted at 2500 rpm for 20 s. The ITO/ZnO/ZnSe sample is first annealed at 150 °C for 3 min and then transferred to another hot plate and annealed at 380 °C for 40 s. The thickness of the ZnSe NCs with a single layer is about 20 nm. To fabricate ZnSe NC film with different thicknesses, the above process is repeated several times until the desired thickness is achieved. To apply the EDT ligand treatment, several drops of 1% EDT methanol solution are put on top of ZnSe NCs and spin casted at 3000 rpm for 20 s to make the ligands exchange their material. Following this, five layers of CdTe NCs with a thickness of about 450 nm are deposited on the substrate using a process similar to the one described previously [21,22]. Finally, several drops of saturated  $CdCl_2$  methanol solution are put on top of the ITO/ZnO/ZnSe/CdTe and spin-casted at 3000 rpm for 20 s. Then the sample is placed in a hot state at 330 °C for 25 min. MoOx (~8 nm) and Au (~80 nm) back contact are deposited in sequence via thermal evaporation by using a shadow mask with an active area of 0.16 cm<sup>2</sup>.

### 2.4. Characterization

The morphology of ZnSe NCs is measured by using transmission electron microscopy (TEM, JEM-2100F, Hitachi, Tokyo, Japan) with a tungsten filament that has an accelerating voltage of 100 kV. The structure of ZnSe NCs is characterized by X-ray diffraction (XRD, X' pert Pro M, Philips, Amsterdam, The Netherlands). The cross-sectional view, the element content, and the structure of NC solar cells are further investigated by using a scanning electron microscope (SEM, NOVA NANO SEM 430, Amsterdam, The Netherlands) equipped with an energy-dispersive spectrometer (EDS) and X-ray diffraction (XRD, X' pert Pro M, Philips, Amsterdam, The Netherlands). Photocurrent density-voltage ( $J$ - $V$ ) measurements are conducted using a Keithley 2400 system and a Xenon Lamp Solar Simulator equipped with an AM 1.5 G filter. The external quantum efficiency spectrum (EQE, Solar Cell Scann100, Zolix Instruments Co., Ltd., Beijing, China) is used to investigate the spectral response of NC solar cells.

### 3. Results and Discussion

The ZnSe NC samples are prepared by injecting TOP-Se into the  $Zn^{2+}$  carboxylic precursor and adopting HDA as the solvent at a high temperature of 300 °C. Using TEM images as shown in Figure 1a, we observe that the ZnSe NCs have a spherical morphology with an average size of ~30 nm. We also found large aggregation, which may be due to the large polarity of ZnSe NC in toluene. The ZnSe NC samples are refluxed in pyridine for 12 h and dried under a vacuum oven at 120 °C for one day before XRD measurement. The diffraction patterns have peaks at about 25.98°, 27.24°, 45.26°, 48.74° and 53.55° as identified from the XRD pattern (Figure 2b), corresponding to the (100), (002), (110), (103) and (112) facets, which agree well with the standard wurtzite structure of ZnSe (JCPDS 97-1463). The ultraviolet (UV) absorption peak is located at 412 nm for ZnSe NC in the toluene solution, which corresponds to 3.0 eV for the ZnSe NC bandgap (calculated from the absorption peak of Figure 1c). It is noted that the bandgap calculated from the absorption peak is not accurate, as NC with different diameters existed in this case. To investigate the transmission and bandgap of sintering NC thin films, ZnSe NC with different thicknesses are deposited onto the ITO/ZnO substrate and annealed at 380 °C for 10 min to remove any organic solvent and impurity. The average thickness of ZnSe NC thin film is measured by using a profilometer. The typical transmission spectra of the ZnSe NC thin films (ITO/ZnO/ZnSe), which have 60 nm, 100 nm, and 120 nm thicknesses, are shown in Figure 1d (inset shows the plot of  $(\alpha h\nu)^2$  versus the photon energy). It is clear that the NC thin films are nearly transparent in a wavelength range higher than 500 nm and the films show high transparency for wavelengths below 450 nm, which is beneficial for light harvesting of the CdTe NC active layer. The transmission decreases in wavelengths below 500 nm with an increased thickness of ZnSe NC. From the inset of Figure 1d, the bandgap of the ZnSe thin film is 2.81 eV, which is derived by taking a tangent of a straight line at  $A = 0$  ( $A = (\alpha h\nu)^2$ ).

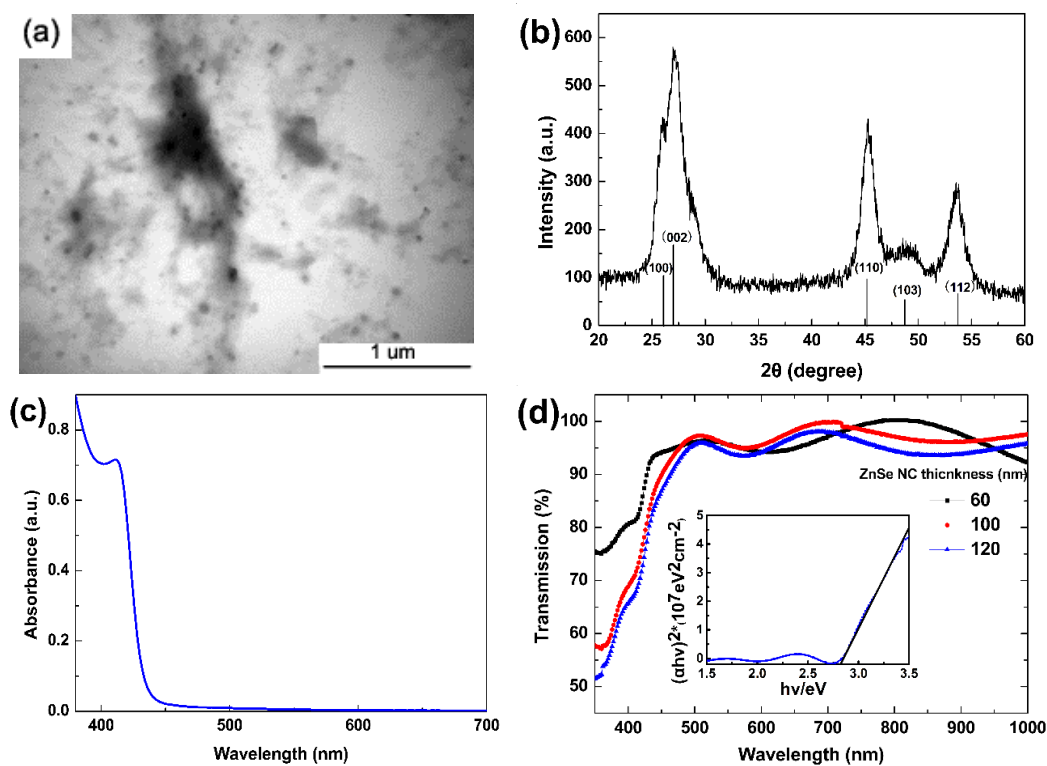


**Figure 1.** (a) Transmission electron microscope (TEM) image of ZnSe nanocrystal (NC); (b) X-ray diffraction (XRD) pattern of the ZnSe NC (nanocrystal) thin film; (c) absorbance of ZnSe NCs in toluene; and (d) transmission spectrum of the ZnSe NC thin film with different thicknesses (ITO/ZnO/ZnSe, inset shows the plot of bandgap).

The architecture and band alignment of the NC device are presented in Figure 2a,b. In this device structure, carriers are mainly generated in the CdTe NC active layer. Unlike CdS or CdSe, the conduction band of ZnSe is higher than that of CdTe, a type I heterojunction is formed for CdTe/ZnSe heterojunction, and therefore band bending at the ZnSe interface is spike like. It is noted that the hole barrier levels for CdTe/ZnSe heterojunction depends on both the valence band levels and the Fermi levels of the CdTe and ZnSe. A small positive conduction-band offset may help maintain good cell efficiency as it created a large hole barrier adjacent to the interface and reduced interface recombination [32–34]. Efficiency up to 11% has been attained in the case of Cu(In,Ga)Se<sub>2</sub> thin-film solar cells with ZnSe buffer layer [35] while >21% efficiency has been achieved for the ZnS buffer layer [36]. Therefore, CdTe NC solar cells with a ZnSe NC buffer layer is expected to obtain efficiency once the CdTe/ZnSe junction quality is improved. The MoO<sub>x</sub> buffer layer blocks electrons and facilitates hole collecting, which was confirmed in the previous report [27]. The cross-sectional SEM image of ITO/ZnO/ZnSe/CdTe/MoO<sub>x</sub>/Au is presented in Figure 2c. It is clear that the CdTe NC and ZnSe NC layers are compact and pin-hole free. The X-ray photoelectron narrow scan (XPS) of Zn 2p and Se 3d spectra levels are presented in Figure 2d, which implies the formation of the ZnSe composite. The thickness of the ZnSe NC buffer layer and the annealing temperature have great impact on the performance of NC solar cells, as shown in Figure 2e, f. To compare device performance with different thicknesses of ZnSe NC, all the samples are prepared at the same conditions and annealed at 350 °C with CdCl<sub>2</sub> treatment after five layers of CdTe NC are deposited. We found that the  $J_{sc}$  increases from 3.58 mA/cm<sup>2</sup> to 10.35 mA/cm<sup>2</sup> when ZnSe thickness increases from 25 nm to 110 nm and decreases to 5.61 mA/cm<sup>2</sup> at 125 nm, which is significantly lower than the thickness among CdTe/CdSe or CdTe/CdS NC solar cells [10,19]. By contrast, the thickness of the ZnSe NC buffer layer has significant effects on the  $V_{oc}$ , FF (fill factor), and PCE of NC solar cells. The efficiency of the NC device is increased from 0.38% to 1.93% when the thickness of ZnSe is increased from 25 nm to 110 nm. In addition, PCE decreases when ZnSe is thicker than 110 nm.

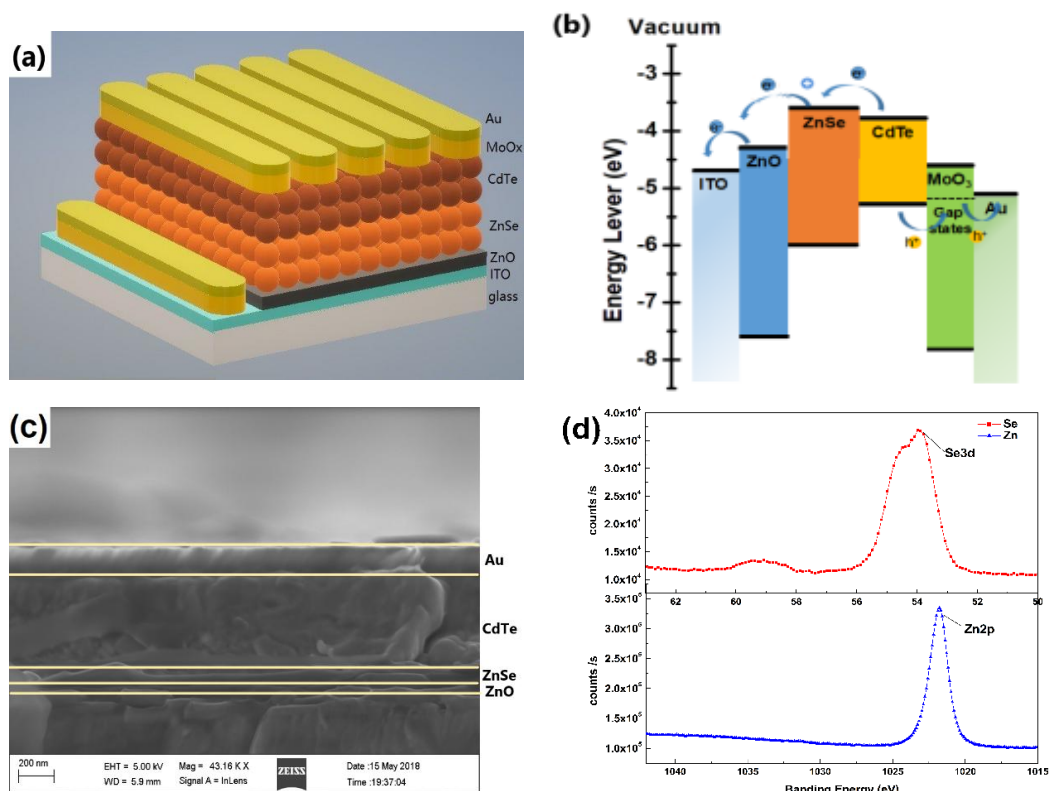
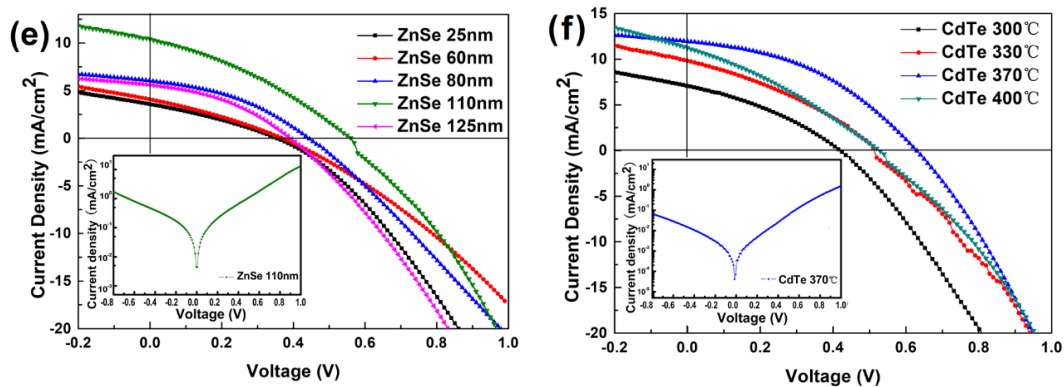


Figure 2. Cont.



**Figure 2.** (a) Schematic and (b) energy band alignment of CdTe NC solar cells with the ZnSe NC buffer layer; (c) cross-sectional scanning electron microscope (SEM) image and (d) X-ray photoelectron narrow scan (XPS) of NC solar cells.  $J$ - $V$  curves of CdTe NC solar cells (e) with different ZnSe NC thicknesses and (f) with different annealing temperatures (inset of Figure 2e,f show the  $J$ - $V$  curve expressed in logarithmic coordinates.).

The best device is obtained when ZnSe is 110 nm with a  $J_{sc}$  of 10.35 mA/cm<sup>2</sup>, a  $V_{oc}$  of 0.56 V, a fill factor (FF) of 33.3%, and a PCE of 1.93%. We observed that low series resistance ( $R_s$ ) is obtained when the ZnSe device has a ~110 nm measurement, which shows that a satisfactory diode performance was obtained. Devices with thin or thick ZnSe NCs show low performance, which may be due to inadequate coverage or a higher thickness with a large series resistor. Annealing has a significant effect on the film and junction quality of NC solar cells. Solar cells are probably affected by changes in the film compactness, junction quality, and any defects existing in the ZnSe/CdTe interface. In the previous report, it was found that the annealing temperature has a significant effect on the CdTe/CdSe NC solar cells. In this study, the influence of the annealing temperature on CdTe/ZnSe device performance is investigated. The  $J$ - $V$  curves of the CdTe solar cells with 110 nm ZnSe annealed at different temperatures are shown in Figure 2f while the detailed parameters are listed in Table 1. The inset of Figure 2e,f show the typical  $J$ - $V$  curve of one device expressed in logarithmic coordinates. CdTe will grow into a larger size (from several nm to ~100 nm) after CdCl<sub>2</sub> annealing, which has been reported in the literature [23]. The formation of larger CdTe grain will reduce grain boundaries and improve carrier collection probability. At a low annealing temperature of 300 °C, the device performance degrades notably due to the low parallel resistance ( $R_{sh}$ ) and the high series resistance ( $R_s$ ). This can be attributed to the imperfect growth of CdTe NC (the grain size of NC is small compared to NC treated at high temperature) at low temperatures, which leads to a large number of defects in the CdTe NC thin film and an increase in the carrier recombination. We also found that device annealing at a higher temperature of 400 °C also results in low device performance due to the decreased  $V_{oc}$  and FF. This may be attributed to the enlarged voids and oxidation of CdTe at high temperatures, which is consistent with the previous report [12]. The solar cells with the ZnSe NCs buffer layer annealed at 370 °C exhibits the best device performance, which includes a  $J_{sc}$  of 11.94 mA/cm<sup>2</sup>, a  $V_{oc}$  of 0.63 V, a FF of 40.79%, and a PCE of 3.07%. This PCE value is ~36% lower than that of the CdTe/ZnSe thin-film solar cells prepared by vacuum technology [28]. In the case of PbS CQDs solar cells, it was found that smooth and low defects NC thin film can be prepared by using the ligands exchanging strategy [37]. In this study, in order to further increase the quality of ZnSe NC film, 1,2-ethanedithiol solution (EDT, 1% v/v in methanol) is adopted during the layer-by-layer processing for developing the ZnSe NC thin film. As shown in Figure 3a, the -SH is firstly bonded to the Zn<sup>2+</sup> of ZnSe NC, then attached to another layer of ZnSe, which permits smooth and compact ZnSe NC film formation during the deposition of ZnSe NC film. From the infrared spectra shown in Figure 3b (transmittance vs. wavenumber), the molecular vibration spectrum corresponding to sulfydryl is found at 559 cm<sup>-1</sup>, 1265 cm<sup>-1</sup> and 2746 cm<sup>-1</sup> respectively for ZnSe NC film coverage with EDT, which implies that EDT is bonded to the

ZnSe NC thin film. The morphologies of the ZnSe NC thin film w/o ligand treatment are characterized by atomic force microscopy (AFM). As shown in Figure 3c,d, the root-mean-square (RMS) roughness for NC with ligand treatment is 4.8 nm while 6.5 nm for NC without ligand treatment. It is also found that without ligand treatment more aggregations are found (Figure 3c), which may result in a large leakage current and low diode quality.

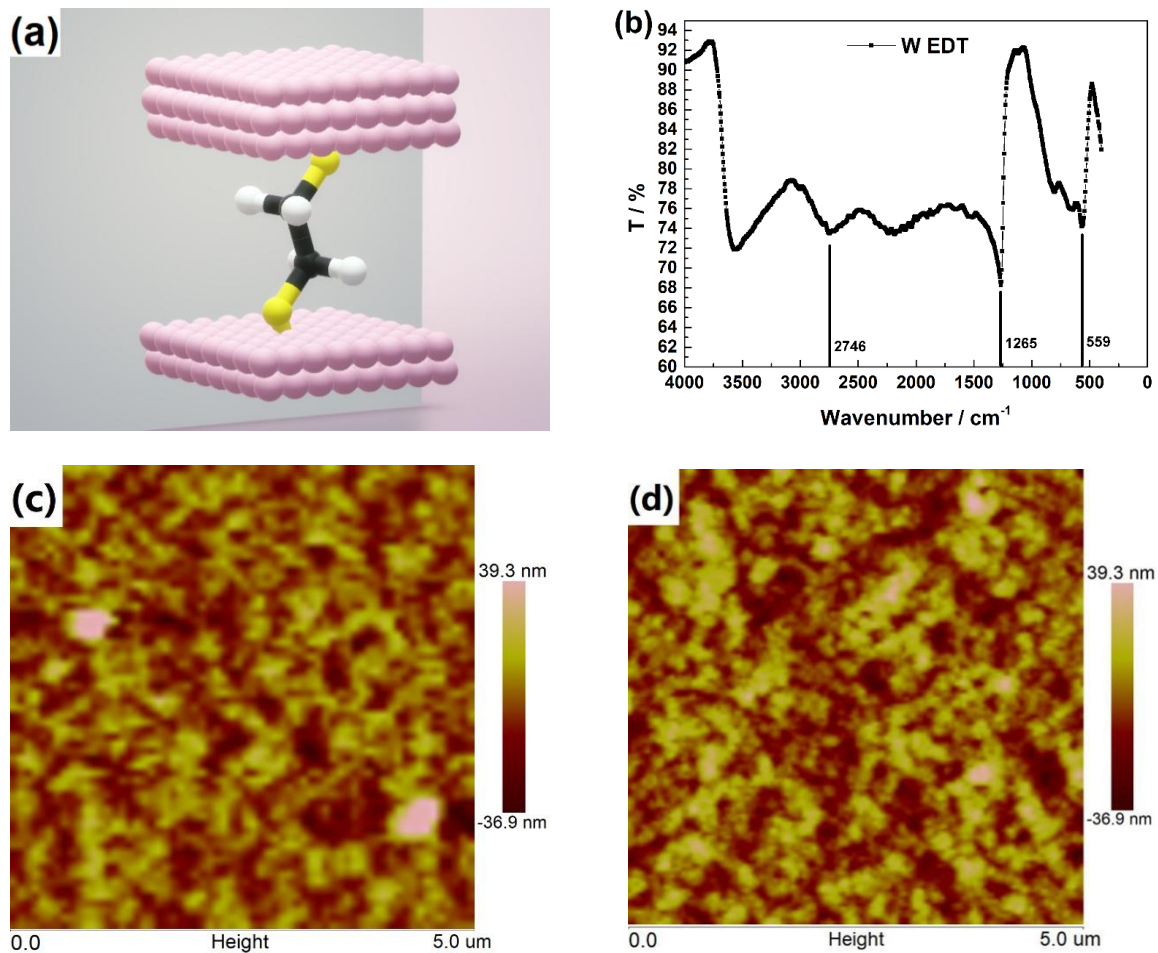


**Figure 3.** (a) A schematic figure of 1,2-ethanedithiol (EDT) bonding to adjacent ZnSe NC film; (b) Infrared spectrum of EDT treated ZnSe NC thin film, atomic force microscopy (AFM) images of ZnSe NC thin film (c) without EDT treatment (d) with EDT treatment.

**Table 1.** Summarized performance of ZnSe/CdTe NC solar cells (FF: fill factor; NCs: Nanocrystals; PCE: Power conversion efficiency, Figure 2e,f).

ZnSe NCs (nanocrystals) Thickness (CdTe NCs Annealing at 350 °C)	$J_{sc}$ (mA/cm <sup>2</sup> )	$V_{oc}$ (V)	FF (%)	PCE (%)	$R_s$ (Ω·cm <sup>2</sup> )	$R_{sh}$ (Ω·cm <sup>2</sup> )
25 nm	3.58	0.40	30.17	0.38	67.56	148.18
60 nm	4.09	0.37	29.96	0.45	64.67	132.51
80 nm	6.03	0.44	38.04	1.02	35.84	219.07
110 nm	10.35	0.56	33.30	1.93	26.08	120.76
125 nm	5.61	0.39	37.83	0.84	33.27	250.40
CdTe NCs annealing temperature (ZnSe thickness 110 nm)						
CdTe 300 °C	7.07	0.41	33.89	0.99	32.9	115.80
CdTe 330 °C	10.35	0.51	33.3	1.70	12.55	106.72
CdTe 370 °C	11.94	0.63	40.79	3.07	23.50	246.15
CdTe 400 °C	11.23	0.53	30.49	1.81	32.32	79.59
1,2-ethanedithiol (EDT) treatment (CdTe NCs annealing at 370 °C with 110 nm ZnSe)						
W EDT	13.55	0.64	47.33	3.58	19.48	251.00
WO EDT	11.94	0.63	40.79	3.07	23.50	246.15

The corresponding  $J$ - $V$  curves characteristic of NC solar cells are presented in Figure 4a. The NC solar cells with ligand treatment have a  $J_{sc}$  of 13.55 mA/cm<sup>2</sup>, a  $V_{oc}$  of 0.64 V, an FF of 47.33%, and a PCE of 3.58%, which is increased by 16.6% in PCE when compared to devices without ligand treatment. From Table 1, it is found that NC solar cells with ligand treatment show a significant improvement in FF (from 40.79% to 47.33%) and  $J_{sc}$  (from 11.94 mA/cm<sup>2</sup> to 13.55 mA/cm<sup>2</sup>) with the  $R_s$  decreasing from 23.50 to 19.48 Ω·cm<sup>2</sup> and the  $R_{sh}$  increasing from 246 to 251 Ω·cm<sup>2</sup>. Therefore, the device with ligand treatment will show less current leaking. It was reported in our previous work that CdTe NC solar cells with efficiency as high as 5.14% are attained with device configuration of ITO/ZnO/CdS/CdTe/MoOx/Au [12]. Comparing these two devices, the low PCE obtained in the ZnSe NC device is mainly attributed to the low  $J_{sc}$  (13.55 mA/cm<sup>2</sup> to 17.26 mA/cm<sup>2</sup> for CdS device) and FF (47.33% to 52.84% for CdS device). It is interesting that the  $V_{oc}$  of the ZnSe NC device is slightly higher than that of the CdS NC device (0.64 V to 0.56 V). Figure 4b shows the  $J$ - $V$  curve in the dark. It is clear that the current density at a reversed bias of  $-1$  V for an EDT treatment device is lower than a device without EDT treatment. However, the reverse and forward current is almost the same at  $V = -0.5$  V and  $V = 0.5$  V. Therefore, EDT treatment can only partly reduce the leakage current and improve the quality of the ZnSe NC film and decrease carrier recombination, which results in improvements for the efficiency of NC solar cells. The EDT treatment techniques here need to be further optimized, such as changing EDT concentration or spin-casting speed, in order to improve the NC solar cells' performance. The external quantum efficiency (EQE) of NC devices without EDT treatment is presented in Figure 4c. It is clear that the EDT treatment device shows a higher EQE response in nearly the whole wavelength than the EQE response in a device without EDT treatment. From the EQE spectrum, one can see that both devices show lower EQE response in the whole wavelength when compared to CdTe NC solar cells with CdS or CdSe NC as buffer layer. We anticipate that the lattice mismatch between CdTe and ZnSe is larger than that of CdTe/CdS or CdTe/CdSe, which will result in low junction quality. Therefore, nonradiative recombination is serious in the interface of CdTe/ZnSe, which will lead to large leakage current and low output short circuit current and device performance. To further increase the performance of CdTe NC/ZnSe solar cells, much work should be done such as optimizing EDT treatment conditions (with different EDT concentration, spin-casting

ratio or using different ligands such as 2-mercaptopropionic acid), using different ZnSe fabricating technics (such as chemical bath deposition, sputtering or evaporation). Furthermore, introducing a very thin layer of CdS or CdSe between CdTe and ZnSe to form graded bandgap solar cells is beneficial for carrier diffusion and collecting. Similar work had been confirmed in the device with configuration of glass/FTO/n-ZnS/n-CdS/n-CdTe/Au [38].

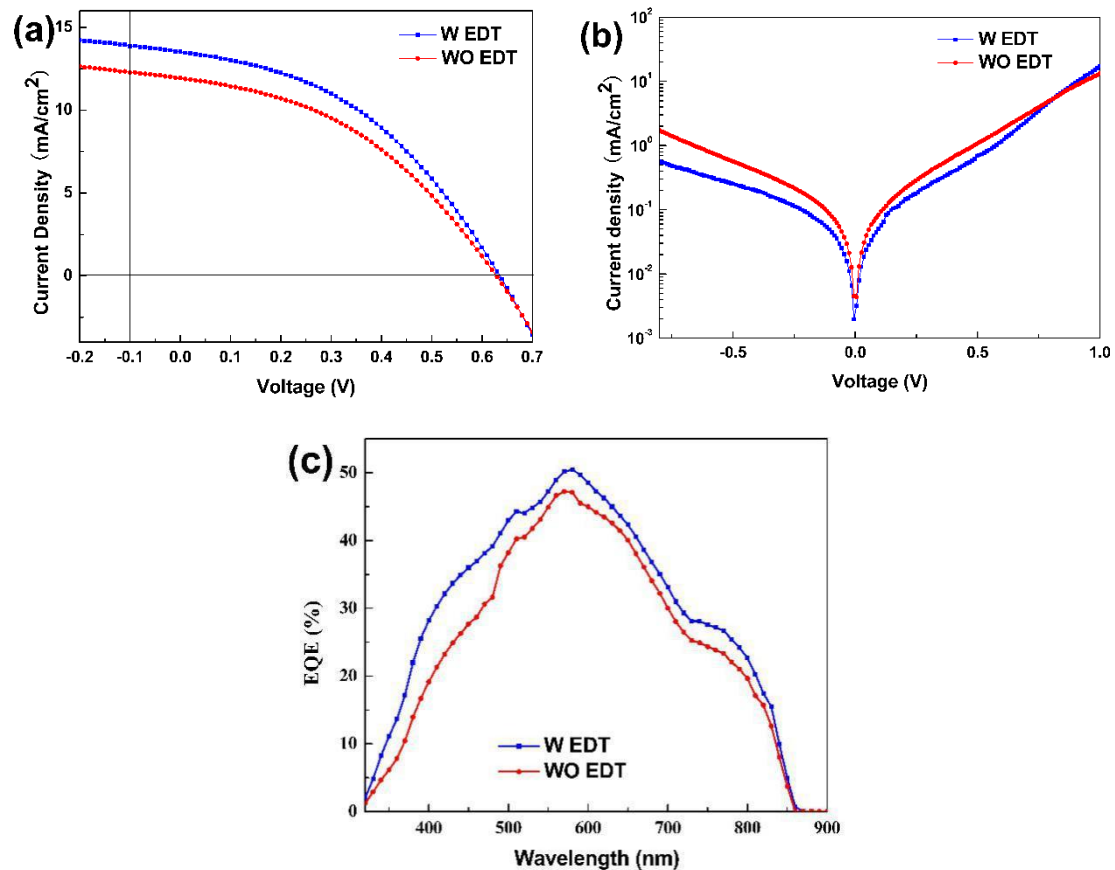


**Figure 4.** *J*-*V* curves of CdTe NC solar cells without EDT treated ZnSe NC film (a) under light and (b) dark; (c) external quantum efficiency (EQE) spectrum.

#### 4. Conclusions

In conclusion, we have introduced a new wide bandgap ZnSe NC as the buffer layer for solution-processed CdTe NC solar cells. The effects of ZnSe thickness and the annealing temperature on device performance have been investigated and discussed. The device with EDT treatment performed on the buffer layer shows an improved PCE of 3.58%, which is 16.6% higher than the device without EDT treatment. Due to the large bandgap and easy fabrication process, CdTe NC solar cells based on the ZnSe NC buffer layer open up a new way for developing low-cost and efficient solar cells.

**Author Contributions:** D.Q. and Y.C. conceived and designed the experiments. Y.C., X.L., X.M., B.W. and J.Y. conducted the experiments. L.H. and Y.C. analyzed the data. W.X., D.W. and J.Y. contributed reagents/materials/analysis tools. W.X., D.Q. and Y.C. compiled the paper.

**Funding:** This research received no external funding.

**Acknowledgments:** We thank the financial support of the National Natural Science Foundation of China (Nos. 91333206, 61774077 and 61274062), the Guangzhou Science and Technology Planning Project (No. 201804010295), the National Undergraduate Innovative and Entrepreneurial Training Program (No. 201710561048), and the Fundamental Research Funds for the Central Universities.

**Conflicts of Interest:** The authors declare no conflict of interest.

## References

1. Lan, X.; Voznyy, O.; Arquer, F.P.G.; Liu, M.; Xu, J.; Proppe, A.H.; Walters, G.; Fan, F.; Tan, H.; Liu, M.; et al. 10.6% Certified Colloidal Quantum Dot Solar Cells via Solvent-Polarity-Engineered Halide Passivation. *Nano Lett.* **2016**, *16*, 4630–4634. [[CrossRef](#)] [[PubMed](#)]
2. Ning, Z.; Ren, Y.; Hoogland, S.; Voznyy, O.; Levina, L.; Stadler, P.; Lan, X.; Zhitomirsky, D.; Sargent, E.H. All-inorganic colloidal quantum dot photovoltaics employing solution-phase-halide passivation. *Adv. Mater.* **2012**, *24*, 6295–6299. [[CrossRef](#)] [[PubMed](#)]
3. Xue, H.; Wu, R.; Xie, Y.; Tan, Q.; Qin, D.; Wu, H.; Huang, W. Recent Progress on Solution-Processed CdTe Nanocrystals Solar Cells. *Appl. Sci.* **2016**, *6*, 197. [[CrossRef](#)]
4. Yang, H.F.; Zhang, J.C.; Zhang, C.F.; Chang, J.J.; Lin, Z.H.; Chen, D.Z.; Xi, H.; Hao, Y. Effects of Annealing Conditions on Mixed Lead Halide Perovskite Solar Cells and Their Thermal Stability Investigation. *Materials* **2017**, *10*, 837. [[CrossRef](#)] [[PubMed](#)]
5. Vivo, P.; Salunke, J.K.; Priimagi, A. Hole-Transporting Materials for Printable Perovskite Solar Cells. *Materials* **2017**, *10*, 1087. [[CrossRef](#)] [[PubMed](#)]
6. Jo, J.; Kim, Y.; Choi, J.M.; de Arquer, F.P.G.; Walters, G.; Sun, B.; Ouellette, O.; Kim, J.W.; Proppe, A.H.; Quintero-Bermudez, R. Enhanced Open-Circuit Voltage in Colloidal Quantum Dot Photovoltaics via Reactivity-Controlled Solution-Phase Ligand Exchange. *Adv. Mater.* **2017**, *29*, 1703627. [[CrossRef](#)] [[PubMed](#)]
7. Wu, C.K.; Sivashanmugan, K.; Guo, T.F.; Wen, T.C. Enhancement of Inverted Polymer Solar Cells Performances Using Cetyltrimethylammonium-Bromide Modified ZnO. *Materials* **2017**, *17*, 378. [[CrossRef](#)] [[PubMed](#)]
8. Gur, I.; Fromer, N.A.; Geier, M.L.; Alivisatos, A.P. Air-stable all-inorganic nanocrystal solar cells processed from solution. *Science* **2005**, *310*, 462–465. [[CrossRef](#)] [[PubMed](#)]
9. Yoon, W.; Townsend, T.K.; Lumb, M.P.; Tischler, J.G.; Foos, E.E. Sintered CdTe Nanocrystal Thin Films: Determination of Optical Constants and Applications in Novel Inverted Heterojunction Solar Cells. *IEEE Trans. Nanotechnol.* **2014**, *13*, 551–556. [[CrossRef](#)]
10. Liu, H.; Tian, Y.Y.; Zhang, Y.J.; Gao, K.; Lu, K.K.; Wu, R.F.; Qin, D.H.; Wu, H.B.; Peng, Z.S.; Hou, L.T.; et al. Solution processed CdTe/CdSe nanocrystal solar cells with more than 5.5% efficiency by using an inverted device structure. *J. Mater. Chem. C* **2015**, *3*, 4227–4234. [[CrossRef](#)]
11. Zeng, Q.; Hu, L.; Cui, J.; Feng, T.; Du, X.; Jin, G.; Liu, F.; Ji, T.; Li, F.; Zhang, H.; Yang, B. High-Efficiency Aqueous-Processed Polymer/CdTe Nanocrystals Planar Heterojunction Solar Cells with Optimized Band Alignment and Reduced Interfacial Charge Recombination. *ACS Appl. Mater. Interfaces* **2017**, *9*, 31345–31351. [[CrossRef](#)] [[PubMed](#)]
12. Green, M.A.; Hishikawa, Y.; Dunlop, E.D.; Levi, D.H.; Hohl-Ebinger, J.; Ho-Baillie, A.W.Y. Solar cell efficiency tables (version 51). *Prog. Photovolt.* **2018**, *26*, 3–12. [[CrossRef](#)]
13. Zhang, H.; Kurley, J.M.; Russell, J.C.; Jang, J.; Talapin, D.V. Solution-Processed, Ultrathin Solar Cells from CdCl<sub>3</sub><sup>−</sup>-Capped CdTe Nanocrystals: The Multiple Roles of CdCl<sub>3</sub><sup>−</sup> Ligands. *Am. Chem. Soc.* **2016**, *138*, 7464–7467. [[CrossRef](#)] [[PubMed](#)]
14. Panthani, M.G.; Kurley, J.M.; Crisp, R.W.; Dietz, T.C.; Ezzyat, T.; Luther, J.M.; Talapin, D.V. High Efficiency Solution Processed Sintered CdTe Nanocrystal Solar Cells: The Role of Interfaces. *Nano Lett.* **2014**, *14*, 670–675. [[CrossRef](#)] [[PubMed](#)]
15. MacDonald, B.I.; Gengenbach, T.R.; Watkins, S.E.; Mulvaney, P.; Jasieniak, J.J. Solution-processing of ultra-thin CdTe/ZnO nanocrystal solar cells. *Thin Solid Films* **2014**, *558*, 365–373. [[CrossRef](#)]
16. Kurley, J.M.; Panthani, M.G.; Crisp, R.W.; Nanayakkara, S.U.; Pach, G.F.; Reese, M.O.; Hudson, M.H.; Dolzhenkov, D.S.; Tanygin, V.; Luther, J.M. Transparent Ohmic Contacts for Solution-Processed, Ultrathin CdTe Solar Cells. *ACS Energy Lett.* **2017**, *2*, 270–278. [[CrossRef](#)]
17. Kumar, S.G.; Rao, K.K. Physics and chemistry of CdTe/CdS thin film heterojunction photovoltaic devices: Fundamental and critical aspects. *Energy Environ. Sci.* **2014**, *7*, 45–102. [[CrossRef](#)]
18. Crisp, R.W.; Panthani, M.G.; Rance, W.L.; Duenow, J.N.; Parilla, P.A.; Callahan, R.; Dabney, M.S.; Berry, J.J.; Talapin, D.V.; Luther, J.M. Nanocrystal grain growth and device architectures for high-efficiency CdTe ink-based photovoltaics. *ACS Nano* **2014**, *8*, 9063–9072. [[CrossRef](#)] [[PubMed](#)]

19. Liu, S.W.; Liu, W.G.; Heng, J.X.; Zhou, W.F.; Chen, Y.R.; Wen, S.Y.; Qin, D.H.; Hou, L.T.; Wang, D.; Xu, H. Solution-processed Efficient Nanocrystal Solar Cells Based on CdTe and CdS Nanocrystals. *Coatings* **2018**, *8*, 26. [[CrossRef](#)]
20. Townsend, T.K.; Foos, E.E. Fully solution processed all inorganic nanocrystal solar cells. *Phys. Chem. Chem. Phys.* **2014**, *16*, 16458–16464. [[CrossRef](#)] [[PubMed](#)]
21. Xie, Y.; Tan, Q.X.; Zhang, Z.T.; Lu, K.K.; Li, M.Z.; Xu, W.; Qin, D.H.; Zhang, Y.D.; Hou, L.T.; Wu, H.B. Improving performance in CdTe/CdSe nanocrystals solar cells by using bulk nano-heterojunctions. *J. Mater. Chem. C* **2016**, *4*, 6483–6491. [[CrossRef](#)]
22. Wen, S.Y.; Li, M.Z.; Yang, J.Y.; Mei, X.L.; Wu, B.; Liu, X.L.; Heng, J.X.; Qin, D.H.; Hou, L.T.; Xu, W.; et al. Rationally Controlled Synthesis of CdSe<sub>x</sub>Te<sub>1-x</sub> Alloy Nanocrystals and Their Application in Efficient Graded Bandgap Solar Cells. *Nanomaterials* **2017**, *7*, 380. [[CrossRef](#)] [[PubMed](#)]
23. Guo, X.Z.; Tan, Q.X.; Liu, S.W.; Qin, D.H.; Mo, Y.Q.; Hou, L.T.; Liu, A.L.; Wu, H.B.; Ma, Y.G. High-efficiency solution-processed CdTe nanocrystals solar cells incorporating a novel crosslinkable polymer as the hole transport layer. *Nano Energy* **2018**, *46*, 150–157. [[CrossRef](#)]
24. Paudel, N.R.; Yan, Y.F. Enhancing the photo-currents of CdTe thin-film solar cells in both short and long wavelength regions. *Appl. Phys. Lett.* **2014**, *105*, 183510. [[CrossRef](#)]
25. Poplawsky, J.D.; Guo, W.; Paudel, N.; Ng, A.; More, K.; Leonard, D.; Yan, Y.F. Structural and compositional dependence of the CdTe<sub>x</sub>Se<sub>1-x</sub> alloy layer photoactivity in CdTe-based solar cells. *Nat. Commun.* **2016**, *7*, 12537. [[CrossRef](#)] [[PubMed](#)]
26. Du, X.; Chen, Z.; Liu, F.; Zeng, Q.; Jin, G.; Li, F.; Yao, D.; Yang, B. Improvement in open-circuit voltage of thin film solar cells from aqueous nanocrystals by interface engineering. *ACS Appl. Mater. Interfaces* **2016**, *8*, 900–907. [[CrossRef](#)] [[PubMed](#)]
27. Li, M.Z.; Liu, X.Y.; Wen, S.Y.; Liu, S.W.; Heng, J.X.; Qin, D.H.; Hou, L.T.; Wu, H.B.; Xu, W.; Huang, W.B. CdTe Nanocrystal Hetero-Junction Solar Cells with High Open Circuit Voltage Based on Sb-Doped TiO<sub>2</sub> Electron Acceptor Materials. *Nanomaterials* **2017**, *7*, 101. [[CrossRef](#)] [[PubMed](#)]
28. Spalatu, N.; Serban, D.; Potlog, T. ZnSe films prepared by the close-spaced sublimation and their influence on ZnSe/CdTe solar cell performance. In Proceedings of the International Semiconductor Conference, Sinaia, Romania, 17–19 October 2011; pp. 451–454.
29. Acharya, S.; Bangera, K.V.; Shivakumar, G.K. Electrical characterization of vacuum-deposited p-CdTe/n-ZnSe heterojunctions. *Appl Nanosci.* **2015**, *5*, 1003–1007. [[CrossRef](#)]
30. Chen, H.S.; Lo, B.; Hwang, J.Y.; Chang, G.Y.; Chen, C.M.; Tasi, S.J.; Wang, S.J.J. Colloidal ZnSe, ZnSe/ZnS, and ZnSe/ZnSeS Quantum Dots Synthesized from ZnO. *J. Phys. Chem. B* **2004**, *108*, 17119–17123. [[CrossRef](#)]
31. Kumar, S.; Nann, T. Shape Control of II–VI Semiconductor Nanomaterials. *Semicond. Nanocryst.* **2006**, *2*, 316–329. [[CrossRef](#)] [[PubMed](#)]
32. Song, T.; Kanevce, A.; Sites, J.R. Emitter/absorber interface of CdTe solar cells. *J. Appl. Phys.* **2016**, *119*, 223004. [[CrossRef](#)]
33. Paul, S.; Grover, S.; Repins, I.L.; Keyes, B.M.; Contreras, M.A.; Ramanathan, K.; Noufi, R.; Zhao, Z.B.; Liao, F.; Li, J.V. Analysis of Back-Contact Interface Recombination in Thin-Film Solar Cells. *IEEE J. Photovolt.* **2018**, *8*, 871–878. [[CrossRef](#)]
34. Hegedus, S.S.; Shafarman, W.N. Thin-Film Solar Cells: Device Measurements and Analysis. *Prog. Photovolt.* **2004**, *12*, 155–176. [[CrossRef](#)]
35. Siebentritt, S.; Kampschulte, T.; Bauknecht, A.; Blieske, U.; Harneit, W.; Fiedeler, U.; Lux-Steiner, M. Cd-free buffer layers for CIGS solar cells prepared by a dry process. *Sol. Energy Mater. Sol. Cells* **2002**, *70*, 447–457. [[CrossRef](#)]
36. Friedlmeier, T.M. Improved Photocurrent in Cu(In,Ga)Se<sub>2</sub> Solar Cells: From 20.8% to 21.7% Efficiency With CdS Buffer and 21.0% Cd-free. *IEEE J. Photovolt.* **2015**, *5*, 1487–1491. [[CrossRef](#)]

37. Kagan, C.R.; Lifshitz, E.; Sargent, E.H.; Talapin, D.V. Building devices from colloidal quantum dots. *Science* **2016**, *353*, aac5523. [[CrossRef](#)] [[PubMed](#)]
38. Dharmadasa, I.M.; Ojo, A.A.; Salim, H.I.; Dharmadasa, R. Next Generation Solar Cells Based on Graded Bandgap Device Structures Utilising Rod-Type Nano-Materials. *Energies* **2015**, *8*, 5440–5458. [[CrossRef](#)]



© 2018 by the authors. Licensee MDPI, Basel, Switzerland. This article is an open access article distributed under the terms and conditions of the Creative Commons Attribution (CC BY) license (<http://creativecommons.org/licenses/by/4.0/>).